The Wide - Range Method to Construct Entire Coexistence Liquid-Gas Curve and to Determine the Critical Parameters of Metals.

ARTICLE *in* THE JOURNAL OF PHYSICAL CHEMISTRY B · AUGUST 2015

Impact Factor: 3.3 · DOI: 10.1021/acs.jpcb.5b06336 · Source: PubMed

2 AUTHORS:

E. M. Apfelbaum

Joint Institute for High Temperatures

49 PUBLICATIONS **325** CITATIONS

SEE PROFILE

Vladimir Sergeevich Vorob'ev

Russian Academy of Sciences

177 PUBLICATIONS **835** CITATIONS

SEE PROFILE

THE JOURNAL OF PHYSICAL CHEMISTRY B

Article

pubs.acs.org/JPCB

The Wide-Range Method to Construct the Entire Coexistence Liquid−Gas Curve and to Determine the Critical Parameters of Metals

E. M. Apfelbaum* and V. S. Vorob'ev

Joint Institute for High Temperatures of Russian Academy of Sciences, Izhorskaya 13, bldg. 2, Moscow 125412, Russia

ABSTRACT: A method to find the liquid−gas critical parameters of metallic elements is offered. It takes into account a nonanalytic behavior in the critical point vicinity and the Clapeyron−Clausius asymptotic behavior at low temperatures. The present approach provides good agreement with experimental data for a wide wealth of non-metallic substances and mercury and alkali metals, where the critical parameters and binodals are known from the measurements. We have also found the critical parameters and binodals for Al, Cu, Fe, and Zr, for which corresponding measurements are yet to be obtained.

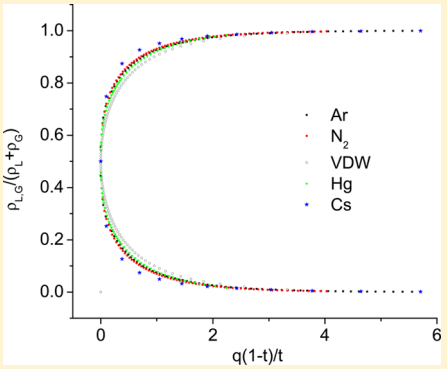

INTRODUCTION

Study of the thermodynamic properties of substances near their liquid−vapor critical points is a challenging problem. Behavior of liquid metals at high temperatures is of particular scientific and technological importance. They are the candidates for high temperature working fluids, e.g., in nuclear reactors, in power converters, and other applications, because they have a high latent heat of vaporization and high heat transfer coefficients. Besides, the states of matter, characterized by high-energy density, occupy a wide region of the phase diagram, for example, hot compressed matter, strongly coupled plasmas, hot expanded liquid, and quasi-ideal plasmas. Our knowledge about these states is limited, because theoretical modeling is complicated and their critical points (CP) appear to be too high for precise experimental study. Only the low temperature binodal branches can be extracted from the measurements. Thus, we have no experimental information concerning the critical parameters for most of the metals (the exceptions are the alkali metals and mercury). Presently there are only theoretical predictions of their critical parameters. A set of different interpolation expressions obtained by a considerable variety of methods is used for CP predictions.[1−3] CP values are required to construct semiempirical equations of state[4] and for the high temperature hydrodynamic calculations.[5] Earlier the universal expression for the description of the liquid and gas branches of the binodal line for a group of real substances was suggested in refs 6−10. The temperature dependence of the gas density along the binodal has a power-law behavior in all of these works. This form of dependence is in disagreement with the Clapeyron−Clausius law according to which the gas density has to decrease exponentially with the temperature decrease. The exponential dependence is a usual way to describe the saturation pressure.[11] However, for the gas density along the binodal, it is not the case. Thus, the methods giving rise to the power-law behavior for the gas density are not valid in the domain of low temperatures. The expression for both binodal branches, which is free from this drawback, is proposed in this paper.

Our consideration is based on the similarity laws and the correspondence (isomorphism) between the lattice models and real substances discussed in recent publications.[12−14] In 1945, Gugenheim[6] showed that for a big group of substances there is some universal dependence between the equilibrium densities of the liquid and vapor and temperatures. One can obviously observe this dependence at the density−temperature plane, if they are written in the coordinates reduced to the critical values (below denoted by subscript "c"). The group includes rare and some molecular gases. The presence of the considered dependence confirms the principle of corresponding states (PCS), one of the most important consequences of the van der Waals equation. Pitzer[8] has formulated a number of assumptions sufficient to lead to PCS. One of them is the statement that PCS can be proved explicitly only if the interaction potentials of the systems can be related by simple scaling transformation of the parameters. For the real systems, the interatomic potential can be very complicated due to the complex structure of molecules and excitation of the electronic degrees of freedom. The latter situation is typical for the liquid metals. The behavior of associative fluids and liquid metals is much more diverse in comparison with the simple molecular fluids. Study of these systems is important in view of the deviation from the classical PCS. In particular, the coexistence

Received: July 2, 2015
Revised: August 2, 2015
Published: August 13, 2015

DOI: 10.1021/acs.jpcb.5b06336
J. Phys. Chem. B 2015, 119, 11825−11832

curves of alkali metals like Cs and Rb have greater asymmetry[15,16] (see, for example, Figure 2 in ref 16). Therefore, there is a wide class of substances for which the classical PCS is violated. Nevertheless, the problem of combining a broad class of substance binodals certainly seems relevant. Clearly, the coordinates ρ/ρ_c and T/T_c are not always suitable for this purpose. (Here ρ/ρ_c and T/T_c are the density and temperature reduced to their critical values.) Appropriate coordinates should combine the binodals for a wider group of substances than PCS does. They also should describe the temperature range from the critical to triple points with acceptable accuracy. To find them is the subject of the present paper. The analogy between real and lattice systems allows one to present the binodal for a substance as a product of symmetric and asymmetric terms. The asymmetric part is the doubled density along the binodal diameter, i.e., $\rho_{2D} = \rho_L + \rho_G$, where ρ_L and ρ_G are the liquid and gas densities. The diameter density, in turn, can also be represented as a sum of two terms. The first one is the ordinary linear term, which is the background for the law of rectilinear diameter common to all fluids. The second one is the nonanalytical term at the CP vicinity, which can be obtained within the renormalization group theory of the critical phenomena.[17] Besides, the proposed expressions for the liquid and gas binodal branches should satisfy accurate results both in the CP vicinity and in the low-temperature limit. Namely, near the critical domain, they should have correct asymptotical form: $|\rho_{L,G} - \rho_c| \sim (1 - T/T_c)^{\beta}$, where ρ_c is the critical density and β is the critical exponent. At $T \to 0$, the gas density dependence should be $\rho_G \sim \exp(-Q/T)$, where Q is some effective heat of vaporization.

The article is organized as follows. In the next section, we will present the expressions for the liquid and gas coexistence curves. Then, we will test the accuracy of the proposed approach for metals with known critical parameters (mercury and alkali metals). The scattering of experimental data will be taken into account as well. We will consider also the CP of metals, for which only the low-temperature parts of binodals were measured. These metals are Al, Cu, Fe, and Zr. Our findings will be compared with the other CP estimates.

EXPRESSION FOR LIQUID AND GAS COEXISTENCE CURVES

It is convenient to present the liquid or gas binodal density by the relation

$$\rho_{L,G} = (\rho_L + \rho_G)\frac{\rho_{L,G}}{\rho_L + \rho_G} = \rho_{2D}x_{L,G} \tag{1}$$

Here ρ_{2D} is the doubled density along the binodal diameter (asymmetrical factor) and $x_{L,G}$ is the symmetrical one because $x_L = 1 - x_G$. The value of $x_{L,G}$ presents also the relative densities along the coexistence curve.[14]

Let us discuss the possible description of the binodal diameter. The general expression for the diameter has been suggested by Fisher and co-workers[18−20] ("complete scaling"). The corresponding relation contains the ordinary linear term $A\tau$ (due to the law of rectilinear diameter common to all fluids) and two nonanalytic terms $B\tau^{2\beta}$ and $C\tau^{1-\alpha}$. Here $\tau = 1 - T/T_c$, as usual. The critical exponents $\beta = 0.326$ and $\alpha = 0.11$ are responsible for the correct behavior in the CP vicinity for real substances.[17] The coefficients A, B, and C in the CP vicinity have been calculated in ref 21. The nonanalytic term $B\tau^{2\beta}$ dominates near the CP, since $2\beta < 1 - \alpha$. Our task is to describe the dependence of ρ_{2D} density on the temperature along the entire (liquid + vapor) coexistence curve from the triple point to the critical point, and not only in the CP vicinity. Thus, we can neglect the less significant term $C\tau^{1-\alpha}$. (Corresponding calculations, accounting for this term, have shown that it has a little effect). Finally, we can present the ρ_{2D} density in the form

$$\rho_{2D} = 2\rho_c + A\tau + B\tau^{2\beta} \tag{2}$$

Here we use another way to determine the coefficients A and B than that in ref 21. To find them, it is possible to consider the asymptotic behavior of ρ_{2D} at low temperatures, when $\tau \to 1$. According to the Clapeyron−Clausius equation, the gas density along the binodal as well as its derivatives tend to zero, i.e., $\rho_G(\tau = 1) = 0$ and $d\rho_G(\tau = 1)/d\tau = 0$. Thus, the values $\rho_{2D}(\tau = 1)$ and $d\rho_{2D}(\tau = 1)/d\tau$ are equal to the values at the liquid binodal branch: $\rho_L(\tau = 1)$ and $d\rho_L(\tau = 1)/d\tau$ correspondingly. The asymptotical properties of the liquid binodal branch at $\tau \to 1$ have been studied earlier.[7,16,22,23] It was shown that the so-called Zeno line is the asymptote to the liquid binodal branch at $\tau \to 1$. (More exactly, it is the asymptote to the continuation of the binodal beyond the triple point.) The Zeno line (ZL or Batchinskii line) has been extensively studied by many researchers.[9,10,16] It is defined as the line where the pressure of a substance P is the same as the pressure of an ideal gas at the same temperature T and density ρ, i.e., the compressibility factor $Z = P/(\rho T) = 1$. ZL has a remarkable property: for a variety of substances, in the density−temperature plane, it is a straight line.[9,10,22] In this plane, ZL starts from the Boyle temperatures T_B at zero densities and crosses the density axis at the Boyle density ρ_B. We should note that the ZL is not always straight (see the limitation in ref 23). However, even in this case, it asymptotically tends to the liquid binodal branch at $\tau \to 1$. Thus, when $\tau \to 1$, the value ρ_{2D} (as well as ρ_L) must tend to ρ_B. Together with eq 2, it leads to the following equality

$$\rho_B = 2\rho_c + A + B \tag{3}$$

The tangent line should also have the same slope as ZL. In the case when ZL is linear, this line is described by the relation[23]

$$\rho_Z = \rho_B(1 - T/T_B) \tag{4}$$

The condition of the coincidence of the tangents has the form

$$\lim_{T\to 0}\frac{d\rho_{2D}}{dT} = \frac{d\rho_Z}{dT} \tag{5}$$

This leads to eq 6

$$A + 2\beta B = T_c\rho_B/T_B \tag{6}$$

The solution of eqs 3 and 6 is

$$A = \frac{\rho_B}{1 - 2\beta}\left[\frac{T_c}{T_B} - 2\beta\left(1 - 2\frac{\rho_c}{\rho_B}\right)\right]$$

$$B = \frac{\rho_B}{1 - 2\beta}\left[1 - 2\frac{\rho_c}{\rho_B} - \frac{T_c}{T_B}\right] \tag{7}$$

The coefficients A and B depend on the Boyle and critical parameters and also on the critical exponent β. If the critical parameters are located along the so-called Z-median,[22] i.e., the line defined by the relation

DOI: 10.1021/acs.jpcb.5b06336
J. Phys. Chem. B 2015, 119, 11825−11832

$$2\frac{\rho_c}{\rho_B} + \frac{T_c}{T_B} = 1 \tag{8}$$

then

$$\rho_{2D} = \rho_B - (1 - 2\rho_c)T/T_c \tag{9}$$

The nonanalytical term disappears in this case. Consequently, the rectilinear diameter law is fulfilled strictly. However, it is more realistic to use the relation between the critical and Boyle parameters in the form

$$\frac{\rho_c}{\rho_B} + \frac{T_c}{T_B} = S \qquad (S \approx 0.67) \tag{10}$$

(see, for example, refs 16 and 23). In this case, the nonanalytical term will be absent, only when $T_c/T_B = \rho_c/\rho_B = S/2$. The latter condition defines the intersection point of the lines determined by eqs 8 and 10.

The symmetrical factor in eq 1, $x_{L,G}$, should provide the correct binodal behavior near the critical point, namely,

$$|x - 1/2| \sim \tau^{\beta} \tag{11}$$

We will use $\beta = 0.326$ for real substances and $\beta = 0.5$ for the van der Waals model.[17,24] On the other hand, at low temperatures, the following asymptotical dependence should take place for the gas binodal density

$$x_G \sim \exp(-q/t), \qquad t \to 0 \tag{12}$$

The value of q in eq 12 corresponds to some effective heat of vaporization Q divided by the critical temperature, i.e., $q = Q/T_c$. We will consider q as a fitting parameter. It should be found from the condition of the minimum error between the calculated density and the experimental (tabulated) data. Then, we can compare the q (or Q) value obtained by this way with the known value of the heat of vaporization at normal conditions Q_0 (i.e., at $P = 1$ atm or at the triple point, when the latter is located at $P > 1$ atm).

Now we can write the expression for $x(t)$, combining the demand of eqs 11 and 12 in the following interpolation formula

$$x_{L,G} = \frac{\rho_{L,G}}{\rho_L + \rho_G} = \frac{1}{2}\left\{1 \pm \left[1 - \exp\left(-\frac{q\tau}{1-\tau}\right)\right]^{\beta}\right\} \tag{13}$$

The positive sign relates to the liquid, while the negative one relates to the gas binodal branches. The corresponding asymptotical behavior of eq 6 is

$$\tau \to 0\text{: } x_{L,G} = \frac{1}{2}\left[1 \pm \left(\frac{q\tau}{1-\tau}\right)^{\beta}\right]$$

$$\tau \to 1\text{: } x_{L,G} = \frac{1}{2}\left[1 \pm \left(1 - \beta \exp\left(-\frac{q\tau}{1-\tau}\right)\right)\right] \tag{14}$$

One can see that the relation $\rho_{L,G}/(\rho_L + \rho_G)$ at fixed β depends only on the factor $q(1-t)/t$. The final expression for the liquid and gas binodals becomes

$$\rho_{L,G} = \frac{\rho_{2D}}{2}\left\{1 \pm \left[1 - \exp\left(-\frac{q\tau}{1-\tau}\right)\right]^{\beta}\right\} \tag{15}$$

where ρ_{2D} is determined by eq 2.

Equations 13 and 15 play the main role in our work. These equations have correct limits at low temperatures and near the CP. Now let us consider these equations for different substances and model systems in the intermediate region.

Before proceeding with the real substances, let us consider possible limitations of eq 15 and its consequences. They rely upon the Zeno-line relations[16,22,23] eqs 4–10. However, these relations can be violated for some substances[16] and models.[23] It is the case for quantum liquids like He and H. Thus, the quantum effects can be one of the possible limitations. Besides, for water and methanol, the Zeno line is not straight. Thus, eq 15 can be incorrect (or at least used with caution) for the cases when the Zeno line is not straight.

COMPARISON WITH TABULATED DATA FOR SUBSTANCES WITH KNOWN CRITICAL PARAMETERS

The binodals for some real nonmetallic substances are available at the NIST database.[25] For metals, the experimental data are presented in refs 26–29 (for alkali metals) and in refs 30 and 31 (for Hg). The Boyle parameters were presented in ref 16.

At first, let us remark the following. The heat of vaporization for real substances and models depends on the temperature. At the critical point, it turns to zero. Therefore, if the value q in eqs 13–15 is considered as some vaporization heat, then it is necessary to define the temperature corresponding to it. The latter point is ambiguous. Therefore, we will proceed as follows. We will consider some value of q^* as a fitting parameter. It should be chosen to obtain the minimum error between the relative density calculated by eq 13 and the tabulated data (the way of minimization is described in the Supplement section). Then, we will compare the q^* value obtained in this way with the known value of heat of vaporization at normal conditions q (i.e., at $P = 1$ atm).

In Figures 1 and 2, we present the test results for argon in the temperature range from the triple to the critical points at $q^* = 5.05$.

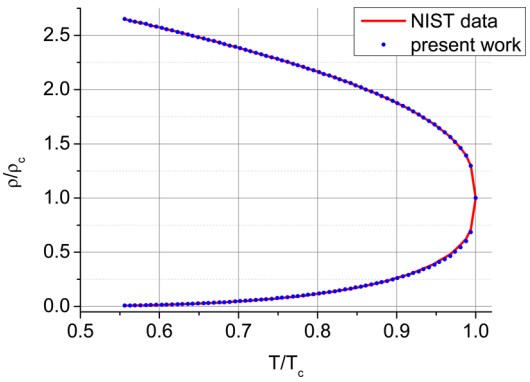

Figure 1. Argon binodal $q^* = 5.05$ ($q = 5.15$). NIST data - ref 25.

Figure 1 demonstrates almost complete coincidence of the table and calculated data. Figure 2 is more informative. It shows that the maximum error of eq 15 is achieved at the temperatures close to the critical one. It is of the order 0.04. The corresponding reduced value of the vaporization heat under normal conditions is equal to $q = 5.15$ (ref 25). The relative difference between q and q^* does not exceed 2%.

Analogously, we have proceeded with the binodal data of some other substances from the NIST database as well as with

DOI: 10.1021/acs.jpcb.5b06336
J. Phys. Chem. B 2015, 119, 11825–11832

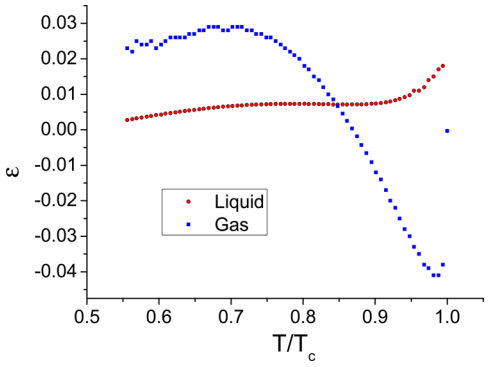

Figure 2. Deviations of the values calculated by eq 15 from tabulated data[25] for argon.

the data for the alkali metals and Hg. Their CP positions and Boyle parameters were presented earlier in ref 16. Besides, we have considered the van der Waals model too. The results are gathered in Tables 1 and 2. For two substances SF_6 and CO_2,

Table 1. Heat of Vaporization[25] and Relative Error ε for the Different Substances and VDW System

substance	Q^a (kJ/mol)	Q (K)	T_c (K)	$q = Q/T_c$	q^*	ε (%)
		Nonmetallic Substances				
Ar	6.45	776.1	150.7	5.15	5.05	3.92
N_2	5.57	670.3	126.2	5.31	5.34	1.12
VDW		27/8	1	3.375	3.47	1.1
O_2	6.82	820.70	154.6	5.31	5.30	3.38
NH_3	23.3	2803.9	405.4	6.92	7.03	3.32
CH_4	8.18	984.4	190.6	5.17	5.17	1.25
CO	6.01	723.2	132.9	5.44	5.43	1.48
CO_2	15.42[b]	1855.7	304.1	6.10	6.59	1.01
C_6H_6	30.83	3710	562.1	6.60	6.60	1.59
H_2S	18.62	2240.7	373.1	6.00	5.79	2.02
N_2O	16.49	1984.4	309.5	6.41	6.23	0.58
SO_2	24.93	3000	430.6	6.97	6.93	3.04
SF_6	15.94[b]	1917.8	318.7	6.02	6.47	0.76
		Metals				
Hg	58.5	7040	1750	4.0	3.9	12
Cs	68.3	6830	1938	4.24	4.85	21
Na	97.9	11780	2500	4.7	5.35	35
K	76.9	17810	2281	4.0	4.5	41
Li	148	3680	17809	4.84	5.8	32
Rb	75.8	9121	2106	4.33	4.25	11

[a]The heat of vaporization at normal pressure P = 1 atm. [b]The heat of vaporization at triple point.

the pressure at any binodal point is more than 1 atm. Therefore, in this case, we have presented the heat of vaporization q at the triple point.

Table 1 shows the heat of vaporization in absolute (Q) and relative units (q) under normal conditions[25] (excluding for SF_6 and CO_2), the values of q^*, as well as the average absolute relative deviation (AARD) denoted as ε. The physical meaning of AARD is the relative error. It is defined in the Supplement section by eq S3. The values of q and q^* are close enough for nonmetallic substances. The AARD for the density along the gas binodal branch does not exceed 4% for these substances. Therefore, the accuracy of eq 15 should be recognized as acceptable to a wide wealth of nonmetallic substances presented in Table 1.

Now let us show that the dependence of $\rho_{L,G}/(\rho_L + \rho_G)$ on $q^*(1 - t)/t$ has the universal character. Figure 3 demonstrates this dependence for some substances from Table 1.

It is evident that the set of the equilibrium curves for different substances is located on the same line described by eq 13. The curve for the VDW equation drops out a little from the general picture due to the other value of the exponent $\beta = 1/2$. The binodals of cesium and mercury are the outermost and innermost, respectively. The binodals of all other substances are located between these ones. In Figure 3, there the binodals for Ar and N_2 only are shown. Similar curves for other substances from Table 1 can be placed between the curves for mercury and cesium and practically coincide with the Ar and N_2 binodals. They are not presented in Figure 3 so as not to clutter it.

Since the measurement of CP parameters and binodals of the alkali metals are few and quite markedly diverge, we have also given them in a separate table, Table 2. As far as the critical pressures P_c for these substances are known, we can also check the Timmermans relation,[32] which is usually used for nonmetallic substances.[7] This relation establishes the link between the critical and Boyle parameters in the following form

$$P_c = \frac{kT_c\rho_c}{m}\frac{\rho_c}{\rho_B} \tag{16}$$

where k is the Boltzmann constant and m is the atomic mass. The relation 16 is initially of semiempirical origin, although there are some theoretical grounds for it.[7]

The experimental results and our calculations are collected in Table 2. The lines in bold indicate the experimental data that have been compared with our calculations. We have chosen the data of ref 31 for mercury and the data of refs 27 and 28 for alkali metals. These data cover a more wide range of temperatures in comparison with data of other references. It is relevant to mention the other CP estimates[33,34] as well. The interaction of atoms in ref 33 was taken into account by means of cohesive energy both for the condensed state and near the critical point. The Monte Carlo numerical simulations with Morse potential were applied in ref 34. The potential parameters were chosen to reproduce the properties of the condensed phase. These data are also included in Table 2.

The experimental data for cesium and mercury are the most reliable as far as them having relatively low critical temperatures. The data of ref 29 for other alkali metals are less reliable, especially along the gas branch of the binodal. As a result, our method gives the smallest error for Hg and Cs. The error along the gas branches for alkali metals is noticeably higher. However, the accuracy of the calculations can be considered acceptable, given the fact that the density along the gas branch of the binodal varies by many orders of magnitude. We note also that the values of calculated q^* correlate with the measured values of q ($q = Q/T_c$, where Q is the heat of vaporization at normal conditions). The experimental and calculated binodals for cesium are presented in Figure 4.

The experimental data[26,28] are close enough to each other. Our binodal corresponds well to the experimental points. AARD on the gas branch is about 20%. It is a relatively small value, as far as the density is changed over 3 orders of magnitude for the considered temperature range. The CP position given in ref 33 overestimates T_c in comparison with the experimental data.

The situation with the other alkali metals is not as favorable as that with cesium. The experimental and calculated binodals

DOI: 10.1021/acs.jpcb.5b06336
J. Phys. Chem. B 2015, 119, 11825−11832

Table 2. Experimental and Calculated Parameters for Alkali Metals

		measured values					calculated values						
Sb	ref	T_c (K)	ρ_c (g/cm^3)	P_c (atm)	q	Z_c	q^*	P_c^* (atm)	ρ_B (g/cm^3)	T_B (K)	Z_c	ε_L (%)	ε_G (%)
Hg	31	1751	5.8	1685	4	0.42	3.9	1685	14.4	6650	0.42	5.2	6.9
Cs	28	1938	0.39	94	4.24	0.2	4.85	94	1.96	4120	0.2	1.2	20
	26	1924	0.38	92.5		0.2							
	33	1950	0.5	450		0.75							
K	27	2281	0.194	164	4.0	0.175	4.5	196	0.93	4660	0.21	11	30
	29	2178	0.17	149		0.19							
	33	2300	0.18	700		0.76							
	34	3120	0.277	534		0.293							
Na	27	2500	0.26	256	4.7	0.14	5.35	381	1.0	5390	0.21	2.5	32
	29	2485	0.175	248		0.159							
	33	2700	0.15	1200		0.85							
	34	3932	0.353	1290		0.26							
Rb	27	2106	0.347	132	4.33	0.19	4.25	153	1.6	4650	0.21	2.5	8.3
	29	2017	0.292	248		0.219							
	33	2250	0.4	650		0.75							
Li	27	3680	0.1	600	4.84	0.137	5.8	803	0.55	7550	0.18	2.6	30
	33	2900	0.05	1400		0.85							

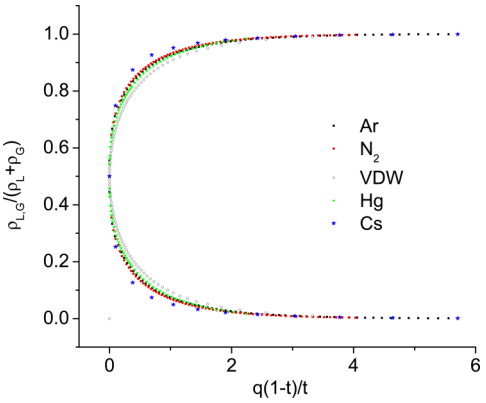

Figure 3. Universal binodal for different substances and the VDW system.

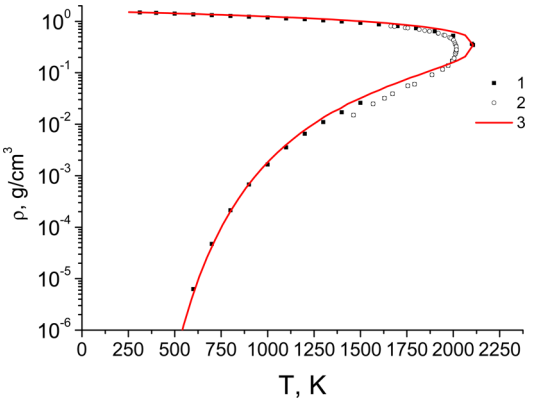

Figure 5. Binodal of Rb. Experiment: 1 - ref 27, 2 - ref 26; 3 - our calculations.

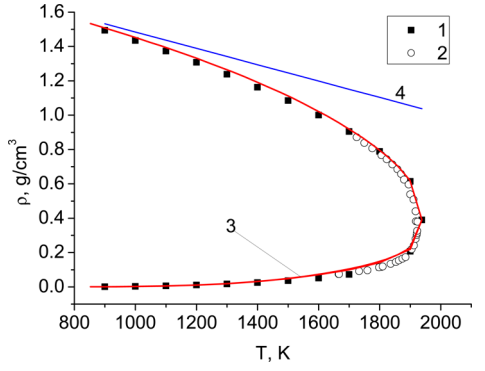

Figure 4. Binodal of Cs. Experiment: 1 - ref 28, 2 - ref 26. Calculations: 3 - our calculations by eq 15, 4 - Z line.

for Rb are plotted in Figure 5 in a logarithmic scale to show the gas density variation.

There is a noticeable difference between experimental data in the critical point region. Our calculations are in good agreement with the experimental points of ref 27.

The relative error (AARD) for the gas branch is equal to 11%. However, the gas density is changed in the case of Rb by 6 orders of magnitude. Consequently, like in the case of Cs, we can consider this accuracy as an acceptable one due to the enormous density range. A similar situation takes place for other alkali metals presented in Tables 1 and 2.

METALS WITH UNKNOWN CRITICAL PARAMETERS

Now we consider a situation when we know (from measurements) the low-temperature branch of the binodals only and there is no information concerning the critical parameters. This is the case for the following metals studied below: Al, Cu, Fe, and Zr. In general, there are no even liquid parts of binodals for these metals, but there are measurements along the isobars in the liquid phase. Compressibility of liquids is generally very low, so the isobars of a liquid are almost coinciding with the liquid binodal branch (see, for instance, Figure 6 in ref 30).

Thus, these isobars can be considered as the parts of binodals without notable errors (see the review in ref 35). Corresponding measurements of density are presented for the temperatures from the triple point to 4−5 kK in refs 35 and 36 for Al and Cu, in refs 37 and 38 for Fe, and in ref 39 for Zr. The saturated vapor pressure data in the same temperature range for a large amount of metals are available from ref 40. Simple approximations describing the data on the vapor pressure are contained in the thermophysical handbooks (for instance, refs 40 and 41). The vapor density is easily determined by the

DOI: 10.1021/acs.jpcb.5b06336
J. Phys. Chem. B 2015, 119, 11825−11832

Table 3. Metals with Unknown CP

	ref	T_c (K)	ρ_c (g/cm^3)	P_c (atm)	Q^a (K)	Z_c	ε_L (%)	ε_G (%)	ρ_B (g/cm^3)	T_B (K)
Cu	this work	7580	1.58	7976	37070* (36654)	0.157	2.4	0.7	8.6	15600
	33	7250	2.3	13500		0.61				
	2	7620	1.4	5770		0.41				
	43	7832	2.13	9034		0.41				
	1	8390	2.39	7460		0.28				
	34	8650	2.63	9543		0.32				
Fe	this work	7928	1.4	2858	42490* (40914)	0.175	3.9	0.01	8.6	16000
	7	7650	1.63	1534		0.2				
	43	8787	2.183	11310		0.34				
	38	9250		8750						
	1	9600	2.03	8250		0.24				
Al	this work	6989	0.365	1057	35854* (34188)	0.137	4.3	2.3	4.6	12900
	7	5500	0.49	1534		0.18				
	42	6299	0.707	884		0.065				
	43	6595	0.698	3988		0.28				
	44	6700								
	33	7400	0.65	8500		0.57				
	1	8000	0.64	4470		0.28				
	34	8472	0.785	5094		0.249				
	2	8860	0.28	4680		0.61				
Zr	this work	9660	2.24	6674	67320* (68231)	0.34	0.2	1.5	0.25	29300

[a]An asterisk denotes the value of the effective heat of vaporization, and the number in parentheses is the heat of vaporization at normal conditions.

saturated vapor pressure, since the vapor for these conditions can be considered as an ideal gas. The Boyle parameters for considered metallic elements (and many other substances) were calculated earlier.[16] Equation 10 allows one to exclude the critical density from eq 15. In this case, the latter equation contains only two unknown parameters, namely, T_c and q. Therefore, the minimization procedure should be carried out with respect to these two values. To verify the procedure, we have applied it to the nonmetallic substances from Table 1. (The details of the procedure and results of the test for nonmetallic substances are presented in the Supplement section.) The obtained results for metals with unknown CP are collected in Table 3.

The earlier estimates of other authors are also included in Table 3. They are shown in order of the T_c increase. Among them, there are the estimates obtained on the basis of similarity relations,[1,2,7,38] deduced from the semiempirical equation of state,[43] obtained by means of "cohesive energy" conception,[33] and resulting from the numerical simulations with Morse potential[33] and the embedded-atom potential.[42] In ref 44, there is the review of various data on T_c for Al, which gives arguments to the authors of ref 44 to estimate the optimal T_c as 6700 K. There is a large scatter between the critical parameters (see also Figures 6 and 7 below). Like in the case of alkali metals, the effective heat of evaporation Q is close to that under normal conditions.

The liquid−gas coexistence curves together with experimental low temperature points for Cu and Al are plotted in Figures 6 and 7 (in logarithmic scale for Cu and linear scale for Al). Our curves are in good agreement with experimental points. (The corresponding errors are shown in Table 3.) The values of CP estimated by other authors are shown in these figures too. The calculations of ref 34 give rise to higher values for the liquid density along the binodal, which are inconsistent with the experimental data at low temperatures. From this point of view, our results are more reasonable.

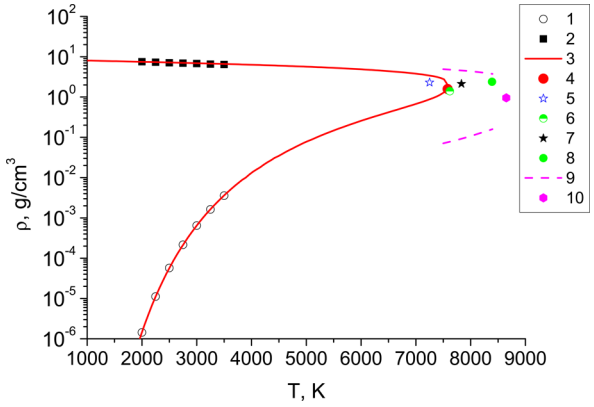

Figure 6. Cu binodal. Experimental data: 1 - gas branch,[40,41] 2 - liquid branch.[35,36] Calculations and estimates: 3 and 4 our binodal and CP, respectively; 5, 6, 7, and 8 are the CP estimates according to refs 33, 2, 3, and 1, respectively; 9 and 10 are the binodal and CP according to ref 34, respectively.

CONCLUSION

We have proposed the expressions for the liquid and gas binodal branches, based on the partition into the symmetric and asymmetric variables. The binodal equation written by means of these variables has both binodal branches symmetrical relative to the binodal diameter. The latter circumstance in turn gives rise to a universal description of coexistence curves of a wide wealth of substances. The corresponding group is much wider than those ones, which satisfy the classical PCS. Both parts take into account the nonanalytic features of the binodal behavior in the CP vicinity required by the renormalization group theory.[17,24] In the low temperature limit, the behavior of the gas binodal corresponds to the Clapeyron−Clausius law, with accuracy up to a pre-exponential factor.

The heat of vaporization found by the minimization of the deviation between the calculated and experimental values correlates well with the heat of vaporization at normal

DOI: 10.1021/acs.jpcb.5b06336
J. Phys. Chem. B 2015, 119, 11825−11832

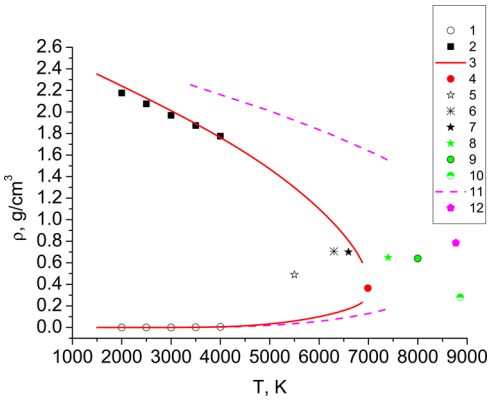

Figure 7. Al binodal. Experimental data: 1 - gas branch,[40,41] 2 - liquid branch.[35,36] Calculations and estimates: 3 and 4 are our binodal and CP, respectively; 5, 6, 7, 8, 9, and 10 are the estimates of CP according to refs 7, 42, 43, 33, 1, and 2, respectively; 11 and 12 are the binodal and CP according to ref 34, respectively.

conditions. To verify the accuracy of the proposed approach, we have constructed the binodals for many nonmetallic substances, mercury and alkali metals, for which the critical parameters were measured. These calculations have shown that the method gives acceptable accuracy both for the liquid and especially for the gas binodal branch, where the density changes by several orders of magnitude. This circumstance has allowed us to build the binodals and find CP coordinates for a number of metals, where analogous measurements are absent. We believe that the values of CP, obtained in this way, are the most reliable of all the previously presented values. The proposed method is simple enough and can be used for other metallic elements, for which there is information on the low-temperature parts of binodals only.

SUPPLEMENT. DETERMINATION OF q AND T_c

Let us consider eq 13. In the general case, the relative densities along the binodals can depend on both q and T_c. To find optimal values of these ones, we can rewrite eq 13 as

$$q\left(\frac{T_c}{T}-1\right)=-\ln\left[1-\left(\frac{\rho_L-\rho_G}{\rho_L+\rho_G}\right)^{1/\beta}\right] \tag{S1}$$

Then, the following functional can be constructed:

$$S(q,T_c)=\sum_{i=1}^{N}\left[X_i^{exp}-q\left(\frac{T_c}{T_i}-1\right)\right]^2$$

Here N is the total number of experimental points and $X_i^{exp}=-\ln[1-((\rho_{L,i}-\rho_{G,i})/(\rho_{L,i}+\rho_{G,i}))_{exp}^{1/\beta}]$ is the value corresponding to the ith experimental point. The minimization of this functional with respect to q and T_c results in the following expressions:

$$T_c=\frac{N\sum_{i=1}^{N}\frac{X_i^{exp}}{T_i}-\sum_{i=1}^{N}\left(\frac{1}{T_i}\right)\cdot\sum_{i=1}^{N}X_i^{exp}}{\sum_{i=1}^{N}\left(\frac{X_i^{exp}}{T_i}\right)\cdot\sum_{i=1}^{N}\left(\frac{1}{T_i}\right)-\sum_{i=1}^{N}\left(\frac{1}{T_i^2}\right)\cdot\sum_{i=1}^{N}X_i^{exp}};$$

$$q(T_c)=\frac{\sum_{i=1}^{N}\frac{X_i^{exp}}{T_i}}{T_c\sum_{i=1}^{N}\frac{1}{T_i^2}-\sum_{i=1}^{N}\left(\frac{1}{T_i}\right)} \tag{S2}$$

Equation S2 allows us to find T_c and q by experimental data.

Using these values, we can calculate an average absolute relative deviation of the calculated density along the binodal from the experimental (or tabulated) one. The average absolute relative deviation (AARD) is defined as $\varepsilon(X)$

$$\varepsilon_a(X)=\frac{1}{N}\sum_{i=1}^{N}\left|\frac{\rho_a^{calc}(T_i,X)}{\rho_a^{exp}(T_i)}-1\right| \tag{S3}$$

where the superscripts "calc" and "exp" mean "calculated" and "experimental" and the subscript "a" means "G" or "L", i.e., the density along the gas or liquid branch of the binodal, respectively. X is a set of parameters that affect the calculated density. If the critical point is known, then $X = q$; if it is unknown, then $X = (T_c, q)$.

We have checked the accuracy of the proposed relation for the nonmetallic substances with known critical points from Table 1. Namely, we have considered only the low temperature part of the corresponding binodal from the triple point T_{tr} to some T_{up}. We have considered two cases: $T_{up} = T_{tr} + (T_c - T_{tr})/2$ (a) and $T_{up} = T_{tr} + (T_c - T_{tr})/3$ (b), i.e., the data along only half and one-third of the binodal, respectively. These segments correspond to the available data range for the metals with unknown critical points (see above). Then, we have applied eq S2 and found the difference between calculated and real T_c. In case a, this difference was less than 1% for all considered gases, while, in case b, it was less than 4%. For instance, in the more undetermined case b, the least error (~0.04%) was for CO_2 (T_{tr} = 216.59 K, T_{up} = 245.77 K, $T_{c,real}$ = 304.13, $T_{c,real}$ = 304.02 K). The maximum error (3.9%) in case b was for O_2 (T_{tr} = 54.361 K, T_{up} = 87.77 K, $T_{c,real}$ = 154.581, $T_{c,real}$ = 148.49 K).

AUTHOR INFORMATION

Notes

The authors declare no competing financial interest.

ACKNOWLEDGMENTS

The work is supported by RFBR grants 14-08-00536, 14-08-00612, and 13-08-12248.

REFERENCES

(1) Fortov, V. E.; Dremin, A. N.; Leont'ev, A. A. Evaluation of the Parameters of the Critical Points. *High Temp.* **1975**, *13*, 984.
(2) Likalter, A. A. Equation of State of Metallic Fluids near the Critical Point of Phase Transition. *Phys. Rev. B: Condens. Matter Mater. Phys.* **1996**, *53*, 4386.
(3) Apfelbaum, E. M.; Vorob'ev, V. S. The Predictions of the Critical Point Parameters for Al, Cu And W Found from the Correspondence between the Critical Point and Unit Compressibility Line (Zeno Line) Positions. *Chem. Phys. Lett.* **2009**, *467*, 318.
(4) Fortov, V. E.; Lomonosov, I. V. Equations of State of Matter at High Energy Densities. *Open Plasma Phys. J.* **2010**, *3*, 122.
(5) Fortov, V. E.; Lomonosov, I. V. Shock Waves and Equations of State of Matter. *Shock Waves* **2010**, *20*, 53.
(6) Guggenheim, E. A. The Principle of Corresponding States. *J. Chem. Phys.* **1945**, *13*, 253.
(7) Filippov, L. P. *Metody rascheta i prognozirovaniya svoistv veshchestv (Methods for Calculating and Predicting the Properties of Substances)*; Moscow State University: Moscow, 1988.
(8) Pitzer, K. S. Some Interesting Properties of Vapor − Liquid or Liquid − Liquid Coexistence Curve for Ionic and Non − Ionic Fluids. *Thermochim. Acta* **1989**, *139*, 25.

DOI: 10.1021/acs.jpcb.5b06336
J. Phys. Chem. B 2015, 119, 11825−11832

(9) Ben-Amotz, D.; Herschbach, D. R. Correlation of Zeno (Z = 1) Line for Supercritical Fluids with Vapor-Liquid Rectilinear Diameters. *Isr. J. Chem.* **1990**, *30*, 59.
(10) Kutney, M. C.; Reagan, M. T.; Smith, K. A.; Tester, J. W.; Herschbach, D. R. The Zeno (Z = 1) Behavior of Equations of State: An Interpretation across Scales from Macroscopic to Molecular. *J. Phys. Chem. B* **2000**, *104*, 9513.
(11) Velasco, S.; Roman, F. L.; White, J. A.; Mulero, A. A Predictive Vapor-Pressure Equation. *J. Chem. Thermodyn.* **2008**, *40*, 789.
(12) Kulinskii, V. L. Simple Geometrical Interpretation of the Linear Character for the Zeno-Line and the Rectilinear Diameter. *J. Phys. Chem. B* **2010**, *114*, 2852.
(13) Kulinskii, V. L. The Critical Compressibility Factor Value: Associative Fluids and Liquid Alkali Metals. *J. Chem. Phys.* **2014**, *141*, 054503.
(14) Apfelbaum, E. M.; Vorob'ev, V. S. The Similarity Relations Set on the Basis of Symmetrization of the Liquid − Vapor Phase Diagram. *J. Phys. Chem. B* **2015**, *119*, 8419.
(15) Hensel, F. Critical Behaviour of Metallic Fluids. *J. Phys.: Condens. Matter* **1990**, *2*, SA33.
(16) Apfelbaum, E. M.; Vorob'ev, V. S. Correspondence between the Critical and the Zeno-Line Parameters for Classical and Quantum Liquids. *J. Phys. Chem. B* **2009**, *113*, 3521.
(17) Fisher, M. E. Renormalization Group Theory: Its Basis and Formulation in Statistical Physics. *Rev. Mod. Phys.* **1998**, *70*, 653.
(18) Fisher, M. E.; Orkoulas, G. The Yang-Yang Anomaly in Fluid Criticality: Experiment and Scaling Theory. *Phys. Rev. Lett.* **2000**, *85*, 696.
(19) Orkoulas, G.; Fisher, M. E.; Ustun, C. The Yang−Yang Relation and the Specific Heats of Propane and Carbon Dioxide. *J. Chem. Phys.* **2000**, *113*, 7530.
(20) Kim, Y. C.; Fisher, M. E.; Orcoulas, G. Asymmetric fluid criticality. I. Scaling with pressure mixing. *Phys. Rev. E: Stat. Phys., Plasmas, Fluids, Relat. Interdiscip. Top.* **2003**, *67*, 061506.
(21) Wang, J.; Anisimov, M. A. Nature of vapor-liquid asymmetry in fluid criticality. *Phys. Rev. E* **2007**, *75*, 051107.
(22) Apfelbaum, E. M.; Vorob'ev, V. S.; Martynov, G. A. Triangle of Liquid-Gas States. *J. Phys. Chem. B* **2006**, *110*, 8474.
(23) Apfelbaum, E. M.; Vorob'ev, V. S. The confirmation of the critical point-Zeno-line similarity set from the numerical modeling data for different interatomic potentials. *J. Chem. Phys.* **2009**, *130*, 214111.
(24) Balescu, R. *Equilibrium and Non-equilibrium Statistical Mechanics*; Wiley-Interscience: New York, 1977.
(25) Lemmon, E. W.; McLinden, M. O.; Friend, D. G. NIST Standard Reference Database #69. In *NIST Chemistry WebBook*; Linstrom, P. J., Mallard, W. G., Eds.; NIST: Gaithersburg, MD, 2004; http://webbook.nist.gov.
(26) Jüngst, J.; Knuth, B.; Hensel, F. Observation of Singular Diameter in the Coexistance Curve of Metals. *Phys. Rev. Lett.* **1985**, *55*, 2160.
(27) Bystrov, P. I.; Kagan, D. N.; Krechetova, G. A.; Shpilrain, E. E. *Liquid Metal Coolants for Heat Pipes and Power Plants*; Hemisphere: New York, 1990.
(28) Vargaftik, N. B.; Gelman, E. B.; Kozhevnikov, V. F.; Naursakov, S. P. Equation of State and Critical Point of Cesium. *Int. J. Thermophys.* **1990**, *11*, 467.
(29) Hensel, F.; Hohl, G. F.; Schaumlffel, D.; Pilgrim, W. C. Empirical Regularities in the Behaviour of the Critical Constants of Fluid Alkali Metals. *Z. Phys. Chem.* **2000**, *214*, 823.
(30) Kikoin, I. K.; Senchenkov, P. Electroprovodnost' i Uravnenie Sostoyaniya Rtuti v Oblasti Temperatur 0 − 200 C I Davlenii 200 − 500 atmosfer (Electrical Conductivity and Equation of State of Mercury for the temperatures 0 − 2000 C and pressures 200 −500 atm). *Fizika metallov i metallovedenie* **1967**, *24*, 843 (in Russian).
(31) Gotzlaff, W. Zustandgleichung und elektrischer transport am kritischen punkt des fluiden quecksilbers. Ph.D. Thesis, University of Marburg, 1988.
(32) Timmermans, J. *Physical - Chemical Constants of Pure Organic Compounds*; Elsevier: Amsterdam, The Netherlands, 1950.
(33) Khomkin, A. L.; Shumikhin, A. S. Critical points of metal vapors. *JETP* **2015**, *148*, 597 (in Russian).
(34) Singh, J. K.; Adhikari, J.; Kwak, S. K. Vapor−Liquid Phase Coexistence Curves for Morse Fluids. *Fluid Phase Equilib.* **2006**, *248*, 1.
(35) Gathers, R. Dynamic Methods for Investigating Thermophysical Properties of Matter at Very High Temperatures and Pressures. *Rep. Prog. Phys.* **1986**, *49*, 341.
(36) Gathers, R. Thermophysical Properties of Liquid Copper and Aluminum. *Int. J. Thermophys.* **1983**, *4*, 209.
(37) Hixson, R. S.; Winkler, M. A.; Hodgson, M. L. Sound Speed and Thermophysical Properties of Liquid Iron and Nickel. *Phys. Rev. B: Condens. Matter Mater. Phys.* **1990**, *42*, 6485.
(38) Beutl, M.; Pottlacher, G.; Jäger, H. Thermophysical Properties of Liquid Iron. *Int. J. Thermophys.* **1994**, *15*, 1323.
(39) Korobenko, V. N.; Savvatimskii, A. I. Svoystva Zhidkogo Zirconiya do 4100 K. (The Properties of Liquid Zirconium up to 4100 K). *Z. Fiz. Khim.* **2003**, *77*, 1742 (in Russian).
(40) Alcock, C. B.; Itkin, V. P.; Horrigan, M. K. Vapor Pressure Equations for the Metallic Elements: 298−2500 K. *Can. Metall. Q.* **1984**, *23*, 309.
(41) Gurvich, L. V.; Veits, I. V.; Medvedev, V. A.; et al. *Termodinamicheskie Svoistva Individual'nykh Veshchestv (Thermodynamic Properties of Individual Substances)*; Izdatel'stvo "Nauka": Moscow, 1978−1982.
(42) Bhatt, D.; Jasper, A. W.; Schultz, N. E.; Siepmann, J. I.; Truhlar, D. G. Critical Properties of Aluminum. *J. Am. Chem. Soc.* **2006**, *128*, 4224.
(43) Lomonosov, I. V. The Phase Diagrams and Thermodynamical Properties of Metals at High Pressures and Temperatures. Doct. Thesis, Institute of Problems of Chemical Physics, 1999 (in Russian).
(44) Morel, V.; Bultel, A.; Cheron, B. G. The Critical Temperature of Aluminum. *Int. J. Thermophys.* **2009**, *30*, 1853.

DOI: 10.1021/acs.jpcb.5b06336
J. Phys. Chem. B 2015, 119, 11825−11832